BIOCHEMISTRY
including biophysical chemistry & molecular biology

ARTICLE

pubs.acs.org/biochemistry

Structural Basis of the RNase H1 Activity on Stereo Regular Borano Phosphonate DNA/RNA Hybrids

Christopher N. Johnson,[†] Alexander M. Spring,[†] Dimitri Sergueev,[§] Barbara R. Shaw,[§] and Markus W. Germann*[,†,‡]

[†]Department of Chemistry and [‡]Department of Biology and Neuroscience Institute, Georgia State University, Atlanta, Georgia 30302-3965, United States

[§]Department of Chemistry, Duke University, Durham, North Carolina 27708, United States

Supporting Information

ABSTRACT: Numerous DNA chemistries for improving oligodeoxynucleotide (ODN)-based RNA targeting have been explored. The majority of the modifications render the ODN/RNA target insensitive to RNase H1. Borano phosphonate ODN's are among the few modifications that are tolerated by RNase H1. To understand the effect of the stereochemistry of the BH_3 modification on the nucleic acid structure and RNase H1 enzyme activity, we have investigated two DNA/RNA hybrids containing either a R_P or S_P BH_3 modification by nuclear magnetic resonance (NMR) spectroscopy. T_M studies show that the stabilities of R_P and S_P modified DNA/RNA hybrids are essentially identical (313.8 K) and similar to that of an unmodified control (312.9 K). The similarity is also reflected in the imino proton spectra. To characterize such similar structures, we used a large number of NMR restraints (including dipolar couplings and backbone torsion angles) to determine structural features that were important for RNase H1 activity. The final NMR structures exhibit excellent agreement with the data (total R^x values of <6%) with helical properties between those of an A and B helix. Subtle backbone variations are observed in the DNA near the modification, while the RNA strands are relatively unperturbed. In the case of the S_P modification, for which more perturbations are recorded, a slightly narrower minor groove is also obtained. Unique NOE base contacts localize the S_P BH_3 group in the major groove while the R_P BH_3 group points away from the DNA. However, this creates a potential clash of the R_P BH_3 groups with important RNase H1 residues in a complex, while the S_P BH_3 groups could be tolerated. We therefore predict that on the basis of our NMR structures a fully R_P BH_3 DNA/RNA hybrid would not be a substrate for RNase H1.

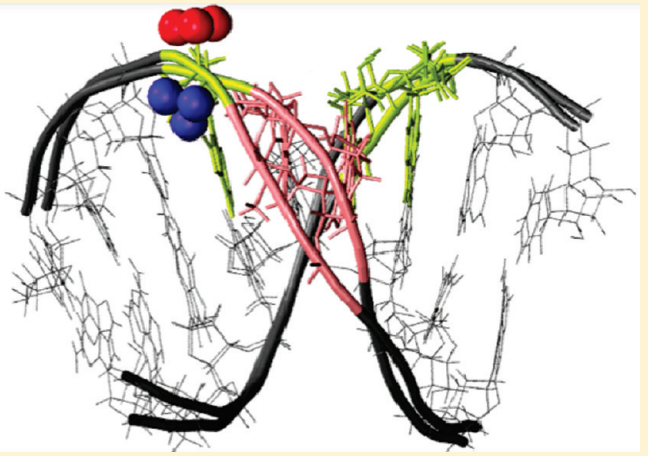

With the advent of antisense technologies more than a decade ago, a number of approaches have been developed for the regulation of gene expression through inhibition via the introduction of a short, RNA complementary DNA oligonucleotide (ODN) and the potential ribonuclease H (RNase H1)-mediated degradation of the RNA strand.[1−3] The challenges with this technique range from increasing the inherently low lipophilicity of the ODN to its degradation by nucleases. Many DNA modifications have been developed in an attempt to circumvent these undesirable properties, which have unfortunately been found to create their own sets of issues, one of the most important being the inability to activate RNase H1. To overcome this, many types of modifications have been explored (methylphosphonates, 2′ modifications, locked nucleic acids, peptide nucleic acids, and morpholino substitutions, among others). While the target affinity has been greatly increased for some of these modifications (PNA and morpholino substitutions, for instance), the resulting hybrids are not substrates for RNase H1.[4−6]

Although binding of an ODN to the mRNA may still silence a gene, RNase H1 activity of an ODN is deemed desirable because it allows a single ODN to mediate the destruction of multiple RNA targets.[7] A recent structure of human RNase H1 in complex with a DNA/RNA duplex has provided insight into the binding process and substrate conformations involved in binding.[8] This has sparked a renewed interest in RNase H1 activity and substrate specificity.

Only a few ODN modifications are able to preserve RNase H1 activity (i.e., phosphorothioate, phosphorodithioate, arabinonucleic acids, and boranophosphates).[9−12] The phosphorothioate

Received: January 18, 2011
Revised: March 24, 2011
Published: March 28, 2011

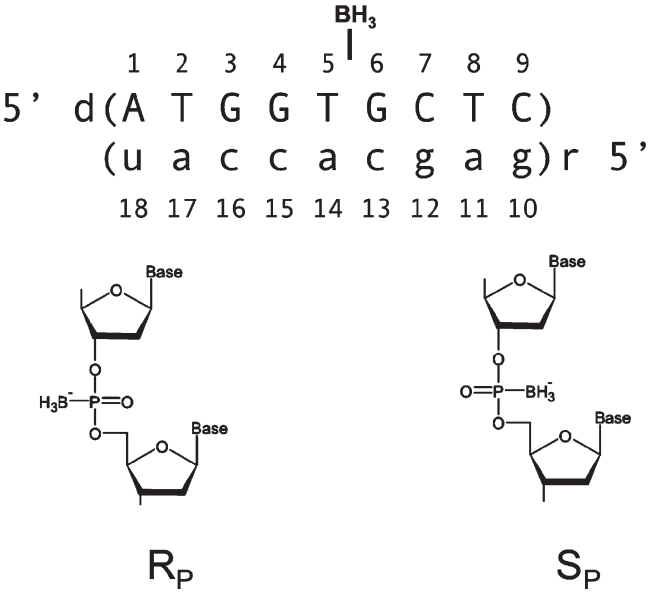

Figure 1. DNA/RNA hybrid design. R_P and S_P denote the chirality of the phosphorus.

diester linkage maintains a pseudo-isoelectronic and isosteric character with a phosphodiester linkage, is relatively easy to synthesize, and maintains canonical sugar and base moieties, but it creates a chiral center at the phosphate linkage. This modification has been found to permit RNase H1 activity yet is resistant to nuclease degradation but suffers from toxicity at higher concentrations, nonspecific interactions with many cellular components, and poor RNA binding.[6] Most other backbone modifications, including methylphosphonates, are not substrates for RNase H1.[3]

Aside from the phosphorothioate, the borano phosphate modification (insertion of a BH_3 group in place of a nonlinking oxygen) has also been shown to maintain RNase H1 activity. Further, it increases lipophilicity while maintaining binding to the targeted mRNA and exhibits a relatively low toxicity. The borano modification has an isosteric relationship with the methylphosphonate group but maintains a negative charge and is isoelectronic with the oxygen of the phosphodiester group. Coupled with minimal toxicity, the borano phosphate diester linkage continues to show promise.[13−15]

Similar to the phosphorothioate modification, the introduction of the borano group creates a chiral center at the phosphorus (Figure 1). Stereoregular studies of phosphorothioate linkages revealed that RNase H1 activity is modulated on the basis of the stereochemistry with the R_P isomer (the sulfur pointing toward the helix) retaining RNase H1 activity while for the S_P isomer the enzymatic activity is reduced as compared to that of the natural phosphodiester linkage.[16] Previous studies have shown that a fully S_P stereospecifically modified borano phosphate (borano group pointing toward the helix) containing an oligonucleotide retains RNase H1 activity.[15,a] To date, R_P ODN's containing a fully modified backbone have not been studied because such ODN's cannot be enzymatically generated and have to be chemically synthesized.[15,17]

Here, we report the high-resolution NMR solution structures of two DNA/RNA duplex nonamers containing a single S_P or R_P borano phosphate modification. This represents the first detailed fine structural analysis of stereoregular borano phosphate modifications. In conjunction with a recently determined crystal structure of human RNase H1 in complex with a DNA/RNA duplex, we provide a rationale for why the S_P hybrid is a substrate for the enzyme while we predict that the R_P hybrid is not.[8]

MATERIALS AND METHODS

The DNA oligonucleotides were synthesized containing a single stereospecific modification (replacement of a nonbridging phosphodiester backbone oxygen with a BH_3 group) at T_5-P-G_6 as previously described.[18,19] Oligonucleotides were purified and characterized by anion exchange, reverse phase chromatography, and mass spectroscopy. The stereochemistry of the borano phosphonate linkages was confirmed by snake venom digestion as described previously.[20] DNA/RNA duplexes were prepared using extinction coefficients derived from the sum of mononucleotides (absorbance at 260 nm, 80 °C, in 10 mM sodium phosphate) as described previously.[21] For all NMR experiments, samples were prepared in 10 mM sodium phosphate, 50 mM NaCl, and 0.1 mM ethylenediaminetetraacetic acid (EDTA). Water samples (90% H_2O/10% D_2O mixtures) included 80 μM DNA/RNA duplex at pH 6.2, and samples in D_2O included ~1.0 mM DNA/RNA duplex at pH* 6.6. For residual dipolar coupling experiments, pf1 bacterial phage was purchased from Asla and prepared as previously described.[22] Prepared pf1 (~53 mg/mL) was added to NMR samples in appropriate aliquots, and a deuterium splitting of 20.8 Hz was observed at 298 K.

Melting Temperature Studies. T_M values were derived from a six-parameter fit of UV melting curves for a series of duplex concentrations ranging from 5 to 50 μM. The enthalpy was obtained from the concentration dependence of the T_M values and entropy. T_M (C_T = 30 μM) and ΔS were calculated using an equation for the biomolecular association of non-self-complementary strands as described previously.[21]

NMR Spectroscopy. NMR experiments were performed on Bruker AMX 600 and Avance 600 spectrometers, using a 5 mm IDTG-600 triple-resonance (Nalorac Corp.) and broadband inverse Bruker probe heads. Acquisition and processing parameters are similar to those described previously[21] with the following exceptions. For experiments in D_2O, NOESY spectra were recorded with mixing times of 50, 150, and 250 ms with an 8 s delay to ensure complete relaxation. $^1H-^{31}P$ correlation (HPCOR)[23] spectra were strip transformed and processed with a shifted sine bell multiplication in both dimensions (SSB = 2). For water experiments, a 1-1 jump and return and a 1-1 jump and return NOESY with a mixing time of 150 ms were used with a 0.3 s delay at 298 and 280 K. Assignment and integration of two-dimensional (2D) spectra were conducted using SPARKY 3.33.[24] ^1H and ^{31}P were referenced to internal DSS and external 85% H_3PO_4 (capillary in D_2O). Constant-time NOESY (CT NOESY) experiments were conducted using a 12 ms REBURP pulse to select the sugar H3′ region.[25] Boron spectra were recorded for ^{11}B (for ^{11}B, spin 3/2 and 80.42% natural abundance, compared to ^{10}B, spin 3 and 19.58% natural abundance) and were referenced to an external standard (0.80 M borate from Tris borate EDTA at 298 K and pH 8.36). Heteronuclear f2 coupled $^{13}C-^1H$ HSQC spectra were recorded for sugars (^{13}C range of 65−105 ppm) and bases (^{13}C range of 125−175 ppm) in the presence and absence of pf1 phage.

Starting Structures. Initial DNA/RNA hybrids were constructed using Amber 9.0's NUCGEN.[26] Using Xleap with a modified parm99 force field (added BH_3 group), a nonbridging oxygen on the DNA backbone between bases T_5 and G_6 was replaced with a borano (BH_3) group to yield two hybrids with a single R_P or S_P configuration. Sodium ions were added to neutralize the phosphodiester backbone, and the systems were solvated with at least 8.0 Å from the edge of the solute to the edge of a box with ~3200 TIP3P water molecules.

Briefly, the BH_3 force field modification was constructed as follows; for the B−P distance, the empirically determined value of 1.91 Å was used.[27] This distance was found to be reproducible using HF 6-31G* energy minimizations. Atomic point charges were derived via an iterative process using Gaussian 03, the AMBER 9.0 RESP module, and RED.[26,28−30] The R_P and S_P conformers utilize the same parameters with the exception of the placement of the BH_3 group. For more details of the derivation of the BH_3 group parameters, see part S6 of the Supporting Information.

Structure Determination. ^{1}H resonances were assigned via 2D ^{1}H NOESY pathways with the assistance of TOCSY and COSY spectra. ^{31}P resonances were assigned on the basis of HPCOR correlation experiments. NOESY cross-peak volumes were integrated in SPARKY using a Gaussian or Sum Over Box method. A percentage error was manually assigned on the basis of the fit residual and visual inspection of a projected cross slice overlaid with the integral trace. For unresolved peaks, a Sum Over Box integration method was used and a higher percentage error was assigned. Peak volumes for base H8 protons were manually scaled to correct for exchange with the deuterated solvent based on the integration of a one-dimensional ^{1}H spectrum recorded with an 8 s delay. Quantitative distance restraints were derived using an iterative RANDMARDI procedure using COMRA, MARDIGRAS,[31,32] and AMBER 9.0 cycles, as described previously.[21] R^x values were calculated in CORMA using correlation times (τ_C) of 2.5, 3.0, 3.5, and 4.0 ns for base and sugar protons. The overall lowest values were obtained for a τ_C of 3.5 ns. DNA sugar pucker and pseudorotation angles were assessed using a graphical method from the Altona lab.[33] $^3J_{H1'-H2'1}$, $^3J_{H1'-H2'2}$, $^3J_{H1'-H3'}$, ΣH1′, and ΣH3′ were measured from ^{31}P decoupled low-flip angle and DQF-COSY experiments. Pseudorotation angles were derived for the dominant form of each deoxyribose and converted to torsion angle NMR restraints using the PUCKER script from Amber 9.0. Because of extensive overlap at multiple temperatures, the sugar puckers at the core of the S_P hybrid (G_4, T_5, and G_6) and R_P hybrid (G_3, G_6) were estimated on the basis of ^{13}C1′ chemical shifts in conjunction with the analysis of the glycosidic torsion angle and base H6/H8 to sugar H3′ NOESY cross-peak intensities.

Backbone ε torsion restraints were derived on the basis of the ratio of peak heights from CT NOESY experiments (^{31}P coupled vs decoupled) as described in ref 25. Broad backbone torsion angle restraints for α, β, γ, and ζ were generated for nucleotides having standard ^{31}P chemical shifts using values from Blackburn et al.[34,35]

Residual dipolar coupling (RDC) restraints were derived from $^1J_{^{13}C-^1H}$ values measured in the f2 dimension in the presence and absence of pf1 ($\Delta^1J_{^{13}C-^1H}$ values ranged from −14 to 15 Hz). All RDC restraints were implemented at the end of the structure generation process by initially minimizing the alignment tensor of the rigid hybrid, followed by fully restrained minimization (rEM) of the whole system. Following RDC implementation, each system (R_P and S_P hybrid) underwent a 6.0 ns fully restrained MD simulation with RDC alignment at 300 K. Snapshots were recorded at a rate of 1 per ps for the final 10 ps and individually minimized to all restraints, yielding a final bundle of structures. Final structures were selected on the basis of Amber energies, restraint violations, and residual dipolar coupling violations. The root-mean-square deviation (RMSD) was calculated for heavy atoms using VMD version 1.9. Structural features and helicoidal parameters were measured using CURVES version 5.1.[36,37]

Table 1. Thermodynamic Properties of DNA/RNA Hybrids Containing a Central R_P or S_P BH_3 DNA Backbone Modification and an Unmodified Control in 10 mM Sodium Phosphate and 50 mM NaCl (pH 6.4)

	T_M[a] (K)	ΔH (kJ/mol^{-1})	ΔS (kJ mol^{-1} K^{-1})	ΔG[b] (kJ/mol^{-1})
R_P hybrid	313.8 (0.2)	265 (6)	0.747 (0.018)	42.6
S_P hybrid	313.8 (0.2)	263 (15)	0.739 (0.043)	42.4
control[c]	312.9 (0.1)	253 (7)	0.706 (0.022)	42.2

[a] T_M values were calculated for a 30 μM duplex. [b] ΔG values are given for 298 K. [c] Control sample from previously published work under similar conditions.[22]

RESULTS

Thermodynamic Stability. UV melting curves of the modified DNA/RNA hybrids were unaffected by the orientation of the BH_3 group. Thermodynamic properties ΔG and T_M were the same for the R_P and S_P hybrids and were comparable to those of an unmodified DNA/RNA hybrid under similar conditions[21] (Table 1). This indicates that neither the orientation nor the presence of a single BH_3 modification impacts the thermodynamic stability.

Base Stacking and Orientation. Chemical shifts (^{1}H, ^{13}C, ^{31}P, and ^{11}B) for the R_P hybrid, S_P hybrid, and unmodified control are listed in part S4 of the Supporting Information.

Upon comparison of the ^{1}H chemical shifts to those of an unmodified DNA/RNA hybrid, both modified hybrids have small differences at the center of the duplex, while the ends remain indifferent to the presence of the BH_3 modification, which is expected (Figure 2). Chemical shifts of the R_P hybrid more closely resembled those of the unmodified control, with only a few variations for the DNA sugars surrounding the modification ($\Delta\Sigma$|sugar ^{1}H's|, T_5 0.32 ppm, G_6 0.23 ppm) (Figure 2). The S_P hybrid displays larger and more extensive chemical shift differences in the sugars ($\Delta\Sigma$|sugar ^{1}H's|, G_4 0.50 ppm, T_5 0.54 ppm) and bases (T_5 ΔH6 0.16 ppm) at the 5′ side of the DNA modification, with moderate differences extending into the RNA strand (standard deviations of <0.004 ppm) (Figure 2).

Complete base H8/H6 to sugar H1′ NOESY pathways for both modified samples support normal base stacking (also supported by thermodynamic data) and are consistent with a right-handed duplex[38] (part S1a,b of the Supporting Information). NOESY cross-peaks with unusual intensities or exchange peaks were not observed among the base or sugar protons, demonstrating that the R_P and S_P modifications do not grossly perturb or induce multiple conformations of the duplex.

Base Pairing. The presence of an imino proton peak generally results from the formation of a stable base pair. At 280 K, we observe all nine imino proton peaks for both modified duplexes, establishing that the BH_3 modification does not disrupt base

pairing (Figure 2). Upon comparison of the imino proton chemical shifts to those of the control hybrid, the R_P hybrid is again similar to the unmodified control while the S_P modification shows a difference at the 5′ side of the DNA (Figures 2 and 3).

Backbone. Unusual phosphorus chemical shifts are a likely indicator for abnormal torsion angles in the nucleic acid helical phosphodiester backbone that may perturb the helical rise, roll, or twist of a duplex.[39] Upon comparison of the phosphorus chemical shifts of a control hybrid with the R_P and S_P modified hybrids, again the R_P hybrid displays less variation from the control (Figure 2). Similar to the trends of the ^{1}H chemical shifts, the S_P hybrid phosphorus chemical shifts are more perturbed, predominantly on the DNA 5′ side of the modification, with effects extending into the RNA strand (c_{15}-P-c_{16}) (Figure 2). As expected, the T_5-P-G_6 sequence is shifted downfield for both modified hybrids (94.00 ppm for R_P and 95.38 ppm for S_P) because of the BH_3 modification[40] (Figure 4).

The ^{11}B spectrum shows a broad peak (coupled to ^{31}P and ^{1}H) for both modified hybrids (−41.43 ppm for R_P and −42.11 ppm for S_P) (Figure 5). Proton decoupling of the boron spectrum reveals the boron phosphorus coupling ($^1J_{BP} \sim 133$ Hz) (Figure 5).

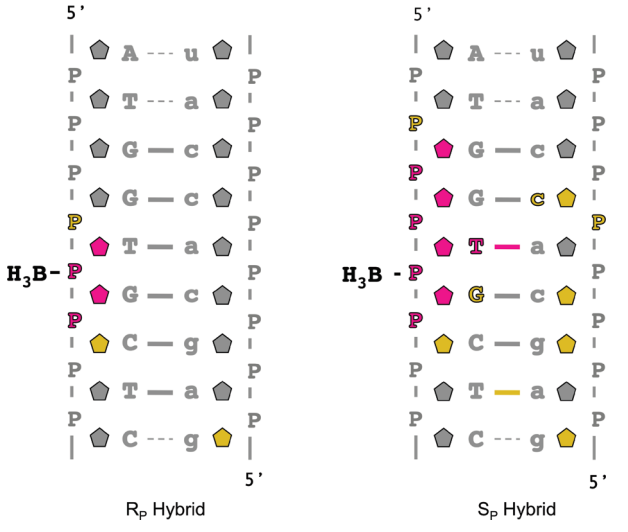

Figure 2. ^{1}H and ^{31}P chemical shift differences at 298 K of the R_P and S_P hybrids compared to an unmodified DNA/RNA control. Each pentagon denotes Σ(|ΔH1′||ΔH2′1||ΔH2′2||ΔH3′|) chemical shifts: P for phosphorus, A, T, G, and C for |ΔH6| or |ΔH8|. Color scheme: magenta for >0.10 ppm differences, yellow for 0.05−0.10 ppm differences, and gray for <0.05 ppm differences. Dashed lines denote imino protons visible at 280 K, and solid lines denote imino protons observed at 298 K.

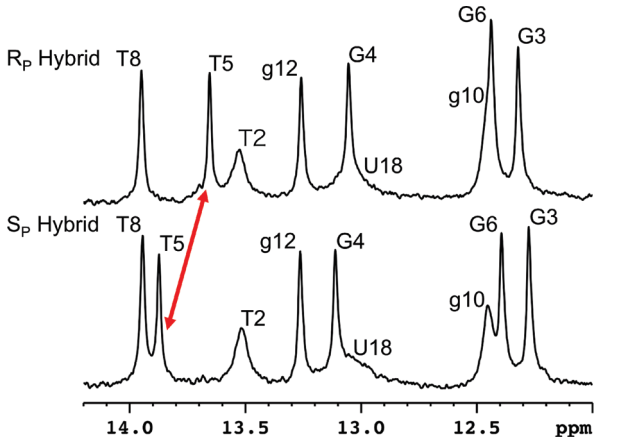

Figure 3. Imino proton spectra of R_P and S_P hybrids (80 μM duplex, 10 mM sodium phosphate, 100 mM NaCl, 0.1 mM EDTA, and 90% H_2O at 280 K and pH 6.2). The red arrow points out the change in the imino proton (T_5) shifts between the two hybrids.

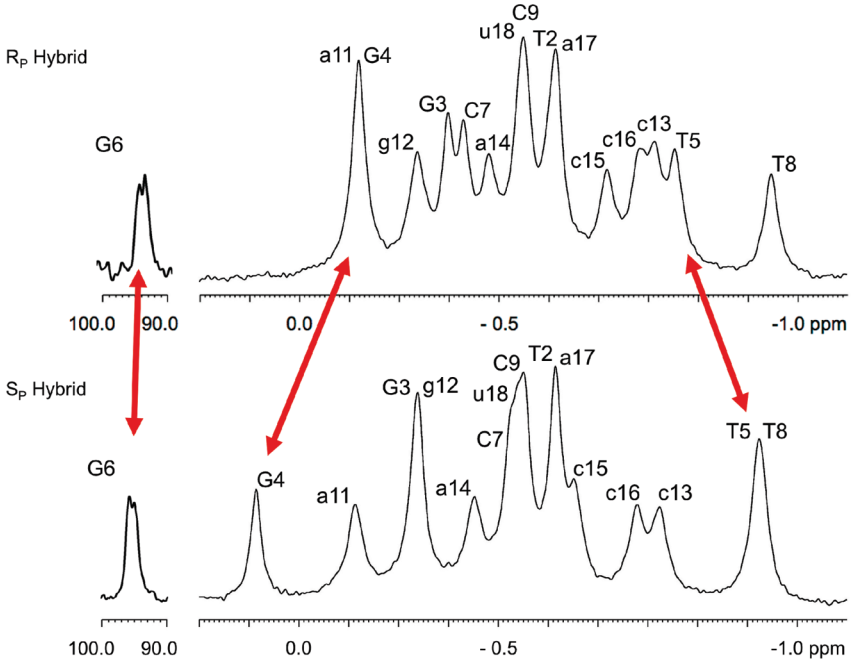

Figure 4. ^{31}P spectra of R_P and S_P hybrids. Assignments were obtained from an HPCOR experiment. Red arrows indicate peaks that have differences of >0.15 ppm between the modified hybrids. The T_5-P-G_6 phosphate experiences a large shift (94 ppm) due to the BH_3 group, similar to other observed ^{11}B−^{31}P chemical shifts.[40]

dx.doi.org/10.1021/bi200083d |*Biochemistry* 2011, 50, 3903–3912

Similarly, in the ^{1}H spectrum, a broad peak is observed for each hybrid from the BH_3 methyl group (0.33 ppm for R_P and 0.42 ppm for S_P) (Figure 5). Decoupling ^{11}B sharpens this peak to a doublet ($^{2}J_{HP}$ = 21.4 Hz), which facilitates the detection of NOE's from the BH_3 group to nearby sugars and bases (Figure 6). The R_P hybrid displays strong NOESY cross-peaks to the surrounding sugars, while for the S_P hybrid, neighboring base contacts are also detected (Figure 6).

The phosphodiester backbone torsion angle ε was determined for the DNA linkages using a CT NOESY experiment.[25] All DNA ε torsion angles were within a standard trans range (−158° to −188°) consistent with B-DNA helical values[35] (part 2 of the Supporting Information). The ε torsion angles that could be determined for the RNA (−145° to −158°) were in line with A-type helical parameters.

Pseudorotation Analysis. The DNA sugar conformation (expressed as fraction south, f_S) was determined from coupling constants $^{3}J_{H1'-H2'1}$, $^{3}J_{H1'-H2'2}$, $^{3}J_{H1'-H3'}$, ΣH1′, and ΣH3′.[33] Because of extensive overlap across a range of temperatures, the f_S at the core of the S_P hybrid (G_4, T_5, and G_6) and G_3 and G_6 of the R_P hybrid was estimated on the basis of ^{13}C1′ chemical shifts in conjunction with analysis of the glycosidic torsion angle and base H6/H8 to sugar H3′ NOESY cross-peak intensities (part 6b,c of the Supporting Information).

The trends in f_S for residues not flanking the modification mimic that of the unmodified control hybrid (parts 3 and 6a of the Supporting Information). The R_P hybrid more closely resembles the unmodified control with moderate changes in f_S for G_4 and T_5. The S_P hybrid likely exhibits larger variations (lower f_S) from the control at G_4 and T_5 based upon the elevated ^{13}C1′ chemical shifts and more intense base−H3′ cross-peaks (part 6a,c of the Supporting Information).

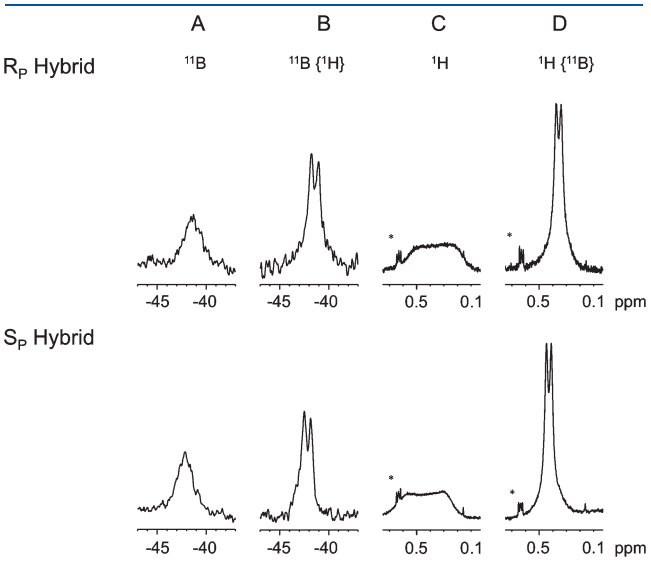

Figure 5. (A) ^{11}B spectra of R_P and S_P hybrids. A single broad peak due to coupling to ^{1}H and ^{31}P is observed (−41.43 ppm for R_P and −42.11 ppm for S_P). (B) Decoupling of ^{1}H sharpens the ^{11}B peak to a doublet ($^{1}J_{BP}$ = 133 Hz). (C) ^{1}H signal of the BH_3 group (0.33 ppm for R_P and 0.42 ppm for S_P). (D) Decoupling of ^{31}P sharpens the ^{1}H signal from the BH_3 modification to a doublet ($^{1}J_{HB}$ = 21.4 Hz). Each asterisk denotes a signal from DSS.

NMR Structure Determination. Both modified hybrid structures are highly restrained (~23 restraints/nucleotide) and exhibit excellent agreement between theoretical and experimental data as evidenced from the low CORMA total R^x values that are less than 6%. The final ensemble of 10 structures, sampled at the end of a 6.0 ns rMD, yields a heavy atom RMSD of <0.35 Å (Table 2 and Figure 7). Amber distance violations were higher for the R_P hybrid (103.9 kcal/mol) than for the S_P hybrid (51.5 kcal/mol); this is largely due to a narrower average well width (0.47 Å vs 0.64 Å) for the quantitative restraints (Table 2). For both structures, the greatest distance penalty was observed for the A_1 H8−A_1 H1′ cross-peak (~8 kcal/mol) and is likely a result of mobility in the adenosine base because of its location at the end of the duplex. All other distance penalties were less than 5.0 kcal/mol (Table 2). Flat angle and torsion angle penalties were negligible (total of <3.5 kcal/mol) for both structures. Residual dipolar coupling alignment data were fit to both structures with excellent agreement, yielding a total alignment constraint of <7.5 kcal/mol (Table 2).

Analysis of the NMR Structures. The single BH_3 DNA backbone modification does not grossly perturb either DNA/RNA hybrid as compared to an unmodified DNA/RNA hybrid[41] (Figure 8 and part 5 of the Supporting Information). Both modified hybrids are fully base paired and right-handed and exhibit a majority of A-type helical properties, similar to those of previously published DNA/RNA hybrid structures.[21,41] All glycosidic bonds are in the anti conformation, and the helical parameters X displacement, Y displacement, incline, rise, and

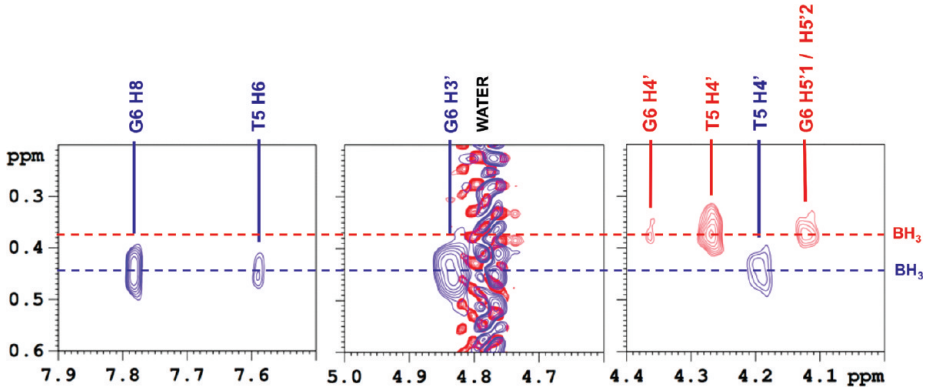

Figure 6. Boron-decoupled {^{11}B} NOESY spectra. The ^{1}H signal from the BH_3 group is sharpened, allowing for the detection of cross-peaks to nearby sugar (R_P hybrid) and base (S_P hybrid) protons. R_P hybrid contacts are colored red and S_P hybrid contacts blue.

Table 2. Summary of NMR Restraints Used for Structure Development[a]

parameter	R_P hybrid	S_P hybrid	force constant (k)[b]
quantitative distance restraints (RANDMARDI)			
no. of nonexchangeable (total)	194	191	30
no. of intraresidue	129	118	30
no. of interresidue (sequential)	56	62	30
no. of interresidue (cross-strand)	2	2	30
average well width (Å)	0.47	0.64	
no. of semiquantitative	5	5	30
average well width (Å)	2.0	2.0	
no. of exchangeable (total)	10	25	10
qualitative BH_3 restraints	2	4	30
endocyclic torsion angle restraints			
no. of deoxyribose (pseudorotation analysis)	35	30	50
average well width ($\lvert r_2 - r_3\rvert/N$)	30	30	
no. of Watson−Crick restraints			
distance	23	23	25
flat angle	23	23	10
backbone torsion angle restraints			
no. of DNA/RNA hybrid broad restraints	70	70	50
well width $\alpha\ \beta\ \gamma\ \zeta$ (deg)	65, 60, 80, 60	65, 60, 80, 60	
ε(C_T NOESY) (deg)	16	16	k varies from 50 to 200 on the basis of the number of data pts
residual dipolar coupling			
total no. of RDC restraints	45	45	1.0 (dwt)
no. of base (C6, C8, C2, C5)	27	27	1.0 (dwt)
no. of sugar (C1′)	18	18	1.0 (dwt)
total no. of restraints	405	427	
total no. of restraints per residue	22.3	23.7	
CORMA R^x	R^x intra, R^x inter, R^x total	R^x intra, R^x inter, R^x total	
T_M = 50 ms	not available	0.057, 0.060, 0.058	
T_M = 150 ms	0.048, 0.050, 0.049	0.060, 0.058, 0.059	
T_M = 250 ms	0.049, 0.065, 0.055	0.055, 0.058, 0.056	
final Amber parameters			
total distance penalty (kcal/mol)	103.9	51.5	
total angle penalty (kcal/mol)	0.5	0.1	
total torsion angle penalty (kcal/mol)	3.4	0.8	
residual dipolar coupling (RDC) alignment constraint (kcal/mol)	7.5	5.3	
Amber energy[b] (kcal/mol)	−210.0	−138.1	
bundle of 10 final structures			
RMSD of heavy atoms (Å)	0.30	0.34	

[a] Quantitative distance restraints were derived using the RANDIMARDI procedure similar to previously published methods.[22] Final restrained molecular dynamic simulations (rMD) were run for 6.0 ns solvated in TIP3P water at 300 K with the addition of Na^+ ions to neutralize phosphate backbone charges. Final ensembles underwent fully restrained minimization (rEM) (1000 steps of steepest descent followed by 1000 steps of a conjugated gradient). The RMSD values were measured in VMD version 1.9. Final Amber energies were calculated in the absence of H_2O and Na^+ ions. [b] In kilocalories per mole.

twist are intermediate between those of canonical A and B helices, with an emphasis toward the A helical form (Table 3 and part 5 of the Supporting Information).

Aligning the heavy atoms of the two hybrids (excluding the BH_3 group) yields an RMSD of 1.19 Å (Figure 8). Qualitative distance restraints involving the BH_3 group point the S_P BH_3 modification into the major groove, while the R_P group extends out from DNA backbone (Figure 8A). On the 5′ side of the modification (bases G_3, G_4, and T_5), the two structures exhibit small differences in the base opening, buckle, and tilt, resulting in a slight bulge in the S_P DNA backbone (Figure 8B). This is also supported by trends in differences in the ^1H, ^{13}C, and ^{31}P chemical shifts and the fact that the only substantial difference in the imino ^1H shift between the two hybrids occurs at T_5. The slight backbone deviation in the S_P hybrid narrows the apparent minor groove, altering the $c_{16}C1'$ chemical shift by 0.8 ppm

(Figure 8B). The ends of the duplex as well as the RNA strands (RMSD for RNA of 0.82 Å) are nearly identical between both modified hybrids and remain indifferent to the BH_3 modification (Figure 8A,B).

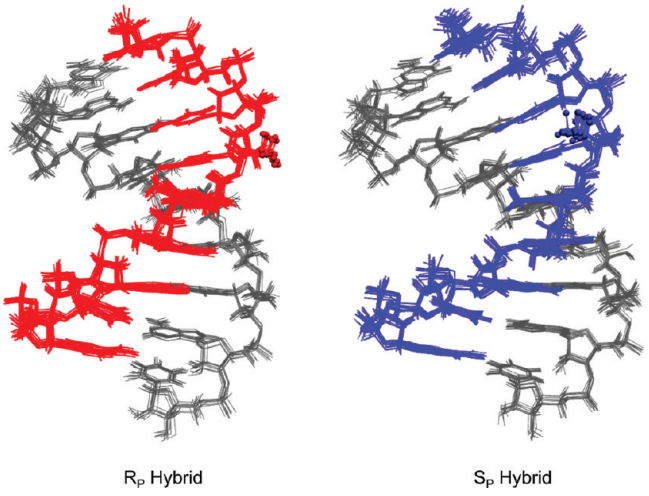

Figure 7. Aligned (heavy atoms) bundles of the 10 final NMR structures. R_P hybrid DNA is colored red, S_P hybrid DNA blue, and RNA gray. Structures were generated by sampling at a rate of 1 per ps for the final 10 ps of a 6.0 ns restrained solvated molecular dynamic simulation (rMD), followed by fully restrained minimization. The RMSD values of the heavy atoms were 0.30 Å for the R_P hybrid and 0.34 Å for the S_P hybrid.

DISCUSSION

RNase H1, an enzyme found in bacteria and humans, degrades the RNA strand of a DNA/RNA hybrid duplex. Earlier studies attempted to utilize the enzyme as a means of regulating protein expression.[42,43] It is now known that RNase H exists in two types (H1 and H2). While RNase H1 may have potential use in gene regulation, unintentional interference with RNase H2 can result in neurological disorders such as Aicardi-Goutieres syndrome.[44]

Previous work from our laboratories has shown that a polynucleotide (15mer) DNA/RNA hybrid containing fully stereospecific (S_P) BH_3-modified DNA backbone linkages maintains RNase H1 activity.[14] Here we provide a rationale for why the BH_3 stereospecific S_P hybrid is a substrate for RNase H1. Two DNA/RNA hybrid NMR solution structures were determined utilizing a large number of restraints (Figure 1). This coupled with the low R^x values permits an analysis of possible fine structural details and subtle features that may impact interactions with the enzyme. The single BH_3 modification is minimally invasive to the overall structure of the DNA/RNA hybrid, with only a slight bulge detected at the 5′ side of the S_P modification. Given the high degree of similarity between the structures and an

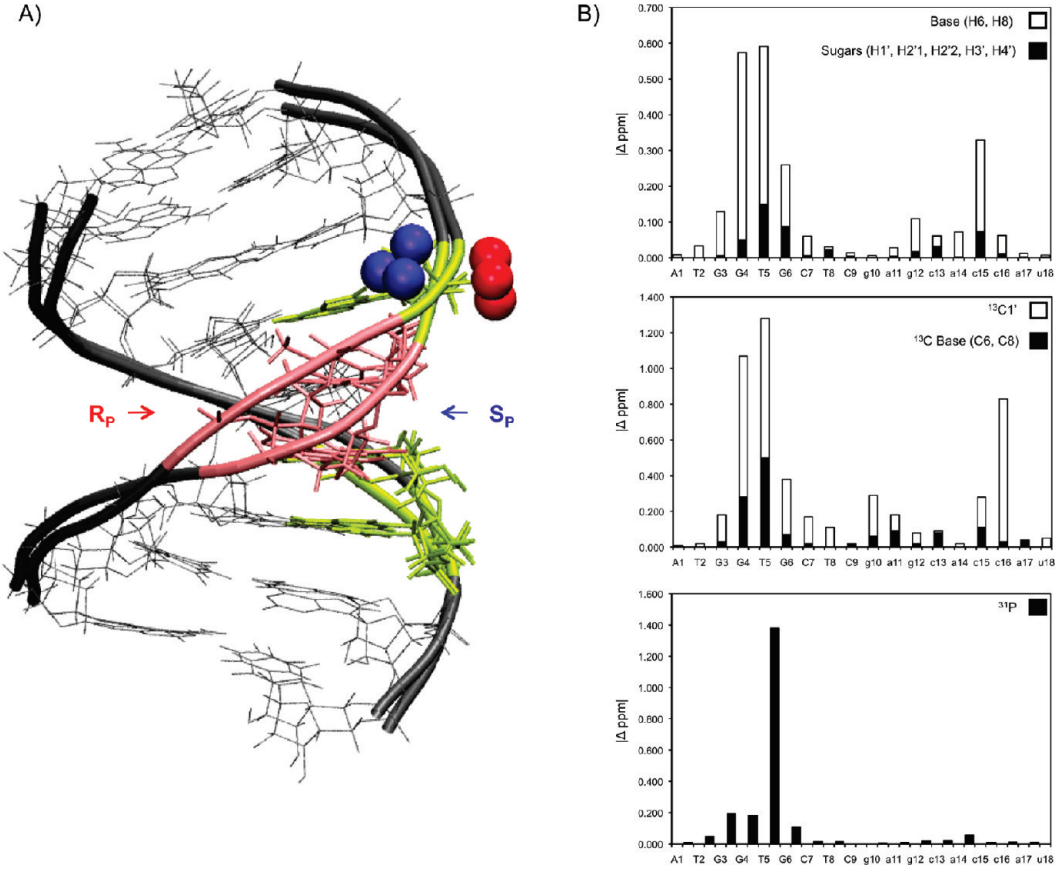

Figure 8. (A) Overlay of R_P and S_P hybrid structures, color-coded according to chemical shift differences between the two modified hybrids. R_P and S_P hybrids aligned by all heavy atoms (except boron). Nucleotides [Σ(|H1′||H2′1||H2′2||H3′||H4′||H6/H8||^{13}C1′||^{13}C6/^{13}C8|)]: magenta for > 1.00 ppm, yellow for 0.50−1.00 ppm, and gray for <0.50 ppm. (B) R_P and S_P hybrid chemical shift difference plotted by residue. ^{1}H (top) closed box denotes Σ(|H1′||H2′1||H2′2||H3′||H4′|), ^{13}C (middle), and ^{31}P (bottom) all in parts per million. The T_5-P-G_6 motif (^{31}P) displays the largest difference in chemical shift between the two modified hybrids (1.2 ppm).

dx.doi.org/10.1021/bi200083d |*Biochemistry* 2011, 50, 3903–3912

Table 3. Selected Helicoidal Parameters for the R_P and S_P Hybrids[a]

	X displacement (Å)		incline (deg)		rise (Å)		twist (deg)	
modified hybrid base pair	R_P	S_P	R_P	S_P	R_P	S_P	R_P	S_P
A-U	−3.1	−3.3	8.8	4.6				
T-A	−3.0	−3.0	13.3	7.4	2.6	2.8	21.8	21.6
G-C	−3.4	−3.4	15.8	11.5	3.0	3.5	39.3	42.8
G-C	−3.3	−3.5	16.0	12.2	2.8	3.0	34.9	36.6
T-A	−3.5	−3.1	18.3	8.9	3.0	2.7	33.7	28.5
G-C	−3.2	−3.0	14.3	7.3	2.9	2.8	37.8	35.0
C-G	−3.3	−3.1	13.8	5.7	2.9	2.8	31.5	28.6
T-A	−3.5	−3.3	15.2	7.1	3.1	3.0	35.8	31.7
C-G	−3.2	−3.0	15.0	8.3	3.1	3.0	35.S	36.9
average	−3.3	−3.2	14.5	8.1	2.9	3.0	33.8	32.7

	X displacement (Å)	incline (deg)	rise (Å)	twist (deg)
A-DNA	−4.1	12	2.9	32.7
B-DNA	0.8	21	3.4	36
DNA/RNA hybrids				
Hantz et al.[42]	−3.3 ± 0.7	10 ± 5	3.1 ± 0.2	33 ± 3
Aramini and Germann[21]	−3.4 ± 0.2	10 ± 2.5	3.0 ± 0.3	32 ± 2

[a] Helical parameters indicate the final NMR structures are similar to an unmodified DNA/RNA hybrid with helical properties between those of A- and B-type helices.

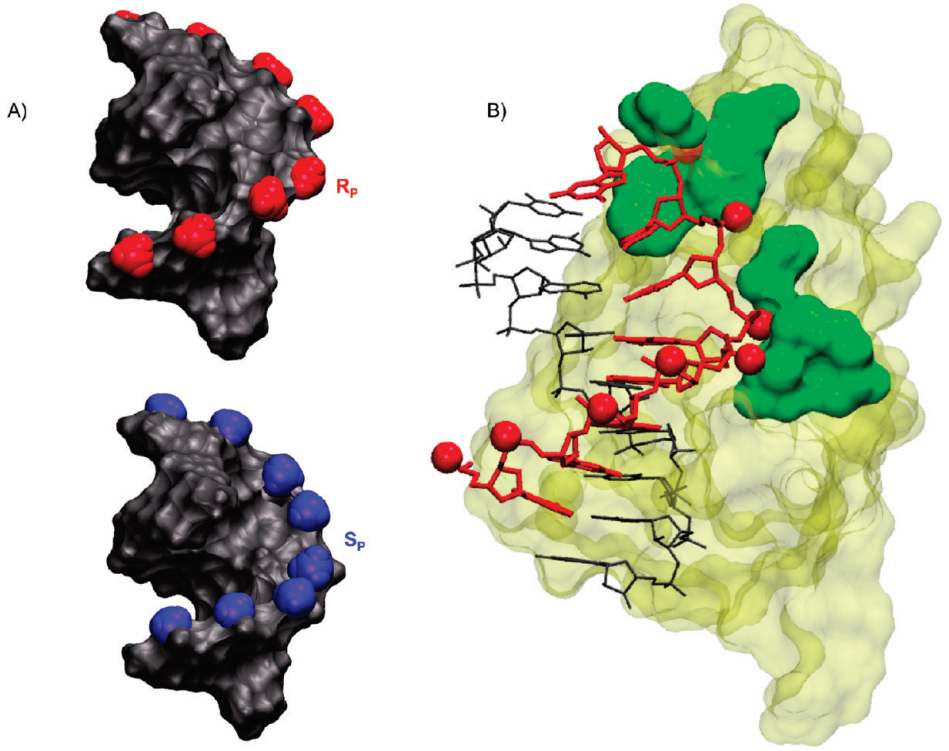

Figure 9. (A) Models of fully stereospecific R_P (red) or S_P (blue) BH_3-modified DNA/RNA hybrids. (B) R_P BH_3 modifications (shown as red CPK spheres) were modeled on the existing crystal structure of RNase H1 (tan) in complex with a DNA (red)/RNA (gray) hybrid.[8] The enzyme contacts the hybrid along the DNA backbone and in the minor groove (green).

unmodified control, the question if they differ in their interaction with RNase H1 arises.

RNase H1 contains two conserved nucleic acid binding domains. The DNA basic protrusion assists in the initial binding of the substrate duplex. The phosphate binding pocket binds the substrate, forms contacts along the DNA backbone, and positions the duplex to place the targeted RNA in the proper location for cleavage. RNase H1 is able to bind both DNA/RNA and

dx.doi.org/10.1021/bi200083d |*Biochemistry* 2011, 50, 3903–3912

RNA/RNA duplexes; however, RNA cleavage occurs for only the DNA/RNA hybrid. The flexibility of the DNA strand permits a snug fit in the phosphate binding pocket that allows the proper placement of the adjacent RNA target strand in the cleavage site. However, in an RNA/RNA duplex, the lack of flexibility and the presence of hydroxyl groups hamper proper binding to the phosphate binding pocket, which displaces the target strand from the cleavage site, resulting in a loss of RNA degradation activity.[8]

As evidenced from our NMR structures, either single modification is well-tolerated in a duplex and results in modest perturbations; therefore, a fully stereospecific modified DNA backbone should not grossly distort a DNA/RNA hybrid. In this context, our structural NMR results provide a rationale for the observed enzyme activity of the S_P BH_3-modified DNA/RNA hybrid.[14] The orientation of the BH_3 plays a critical role in avoiding steric clashes with essential RNase H1 contacts. In the S_P hybrid, the BH_3 group points away from the enzyme surface into the major groove, allowing the DNA strand access to the RNase H1 phosphate binding pocket (Figure 9). Examination of our NMR structures together with the crystal complex[8] predicts that the enzyme can accommodate the S_P orientation of a fully BH_3-modified DNA backbone and maintain RNA cleavage activity. This is in line with experimental data. In the case of the R_P hybrid, the BH_3 modification would obstruct the required snug fit of the DNA into the enzyme's phosphate binding pocket (Figure 9). Additionally, changes in the local charge distribution compared to a regular phosphodiester linkage may also play a role in modulating the enzyme binding affinity. Taken together, these results indicate that the R_P BH_3 group is likely to impede access to essential enzyme binding contacts, thus resulting in the loss of RNase H1 RNA cleavage activity (Figure 9).

■ ASSOCIATED CONTENT

Supporting Information. Tables of ^1H, ^{11}B, ^{13}C, and ^{31}P NMR resonance assignments for the R_P, S_P, and control hybrids, NOESY base H6/H8 to H1′ pathways, ε torsion angles for the R_P and S_P hybrids, H1′—H2′1 and H1′—H2′2 aligned low-flip angle COSY spectra, plots of selected helical parameters of the final R_P and S_P hybrid structures, summary sugar puckering plots for the R_P and S_P hybrids, description of the BH_3 Amber force field modification methodology, and Amber 9.0 and REDCAT back-calculated RDC values and plots as compared to experimentally determined RDC values. This material is available free of charge via the Internet at http://pubs.acs.org.

Accession Codes

Coordinates and NMR-derived restraints have been deposited in the Protein Data Bank (entry 21ar for the R_P hybrid and entry 21b4 for the S_P hybrid) and Biological Magnetic Resonance Bank (entry 17535).

■ AUTHOR INFORMATION

Corresponding Author

*Phone: (404) 413-5561. Fax: (404) 413-5505. E-mail: mwg@gsu.edu.

Funding Sources

This work was supported by National Institutes of Health Grant AI/GM47459 and the Georgia Cancer Coalition. C.N.J. and A.M.S. were supported by the Brain and Behavior and Molecular Basis of Disease programs at Georgia State University, respectively.

Notes

[a]The stereochemistry of phosphorothioate R_P is equivalent to that of borano phosphate SP because of the lower priority of boron as compared to oxygen and sulfur.

■ ABBREVIATIONS

ODN, oligodeoxynucleotide; RNase H1, ribonuclease H; HPCOR, $^1H—^{31}P$ correlation; CT NOESY, constant-time NOESY; rEM, restrained energy minimization.

■ REFERENCES

(1) McClorey, G., Moulton, H. M., Iversen, P. L., Fletcher, S., and Wilton, S. D. (2006) Antisense oligonucleotide-induced exon skipping restores dystrophin expression in vitro in a canine model of DMD. *Gene Ther. 13*, 1373–1381.

(2) Nicholas, M. D., and MCKAY, R. (1994) Inhibition of protein kinase Cα expression in mice after systemic administration of phosphorothioate antisense oligodeoxynucleotides. *Proc. Natl. Acad. Sci. U.S.A. 91*, 11762–11766.

(3) Stein, C. A. (2000) Is irrelevant cleavage the price of antisense efficacy? *Pharmacol. Ther. 85*, 231–236.

(4) Egli, M., Minasov, G., Tereshko, V., Pallan, P. S., Teplova, M., Inamati, G. B., Lesnik, E. A., Owens, S. R., Ross, B. S., Prakash, T. P., and Manoharan, M. (2005) Probing the Influence of Stereoelectronic Effects on the Biophysical Properties of Oligonucleotides: Comprehensive Analysis of the RNA Affinity, Nuclease Resistance, and Crystal Structure of Ten 2′-*O*-Ribonucleic Acid Modifications. *Biochemistry 44*, 9045–9057.

(5) Spurgers, K. B., Sharkey, C. M., Warfield, K. L., and Bavari, S. (2008) Oligonucleotide antiviral therapeutics: Antisense and RNA interference for highly pathogenic RNA viruses. *Antiviral Res. 78*, 26–36.

(6) Kurreck, J. (2003) Anitsense Tehnologies. *Eur. J. Biochem. 270*, 1628–1644.

(7) Aramini, J. M., Van de Sande, J. H., and Germann, M. W. (1998) Structure and Stability of DNA Containing Inverted Anomeric Centers and Polarity Reversals. In *Molecular Modeling of Nucleic Acids* (Leontis, N. B., and SantaLucia, J., Jr., Eds.) pp 92—105, ACS Symposium Series 682, American Chemical Society, Washington, DC.

(8) Nowotny, M., Gaidamakov, S. A., Ghirlando, R., Cerritelli, S. M., Crouch, R. J., and Yang, W. (2007) Structure of Human RNase H1 Complexed with an RNA/DNA Hybrid: Insight into HIV Reverse Transcription. *Mol. Cell 28*, 264–276.

(9) Stein, C. A., Subasinghe, C., Shinozuka, K., and Cohen, J. S. (1988) Physicochemical properties of phosphorothioate oligodeoxynucleotides. *Nucleic Acids Res. 16*, 3209–3221.

(10) Cummins, L., Graff, D., Beaton, G., Marshall, W. S., and Caruthers, M. H. (1996) Biochemical and Physicochemical Properties of Phosphorodithioate DNA. *Biochemistry 35*, 8734–8741.

(11) Rait, V. K., and Shaw, B. R. (1999) Boranophosphates support the RNase H cleavage of polyribonucleotides. *Antisense Nucleic Acid Drug Dev. 9*, 53–60.

(12) Noronha, A. M., Wilds, C. J., Lok, C. N., Viazovkina, K., Arion, D., Parniak, M. A., and Damha, M. J. (2000) Synthesis and Biophysical Properties of Arabinonucleic Acids (ANA): Circular Dichroic Spectra, Melting Temperatures, and Ribonuclease H Susceptibility of ANA·RNA Hybrid Duplexes. *Biochemistry 39*, 7050–7062.

(13) Wang, J. X., Sergueev, D. S., and Shaw, B. R. (2005) The Effect of a Single Boranophosphate Substitution with Defined Configuration on the Thermal Stability and Conformation of a DNA Duplex. *Nucleosides, Nucleotides Nucleic Acids 24*, 951–955.

(14) Wang, X., Dobrikov, M., Sergueev, D., and Shaw, B. R. (2003) RNase H Activation by Stereoregular Boranophosphate Oligonucleotide. *Nucleosides, Nucleotides Nucleic Acids 22*, 1151–1153.

(15) Li, P., Sergueeva, Z. A., Dobrikov, M., and Shaw, B. R. (2007) Nucleoside and oligonucleoside boranophosphates: chemistry and properties. *Chem. Rev. 107*, 4746–4796.

(16) Koziolkiewicz, M., Krakowlak, A., Kwinkowski, M., Boczkowska, M., and Stec, W. J. (1995) Stereodifferentiation the effect of P chirality of oligo(nucleoside phosphorothioates) on the activity of bacterial RNase H. *Nucleic Acids Res. 23*, 5000–5005.

(17) Naoki, I., Natsuhisa, O., and Takeshi, W. (2009) Stereocontrolled synthesis of oligodeoxyribonucleoside boranophosphates via stereodefined H-phosphonate intermediates. *Nucleic Acids Symp. Ser. 53*, 9–10.

(18) Anup, S., Shaw, B. R., and Spielvogel, B. F. (1990) Boron-Containing Nucleic Acids. 2. Synthesis of Oligodeoxynucleoside Boranophosphates. *J. Am. Chem. Soc. 112*, 9000–9001.

(19) Shaw, B. R., Madison, J., Sood, A., and Spielvogel, B. F. (1993) Oligonucleoside boranophosphates (borane phosphonate). *Methods Mol. Biol. 20*, 225–243.

(20) Li, H., Huang, F., and Shaw, B. R. (1997) Conformational Studies of Dithymidine Boranomonophosphate Diastereoisomers. *Bioorg. Med. Chem. 5*, 787–795.

(21) Aramini, J. M., and Germann, M. W. (1999) Solution Structure of a DNA RNA Hybrid Containing an a Anomeric Thymidine and Polarity Reversals: d(ATTGG-3′-3′-aT-5′-5′-GCTC)·r(gagcaccau). *Biochemistry 38*, 15448–15458.

(22) Aramini, J. M., Cleaver, S. H., Pon, R. T., Cunningham, R. P., and Germann, M. W. (2004) Solution Structure of a DNA Duplex Containing an a Anomeric Adenosine: Insight into Substrate Recognition by Enodnuclease IV. *J. Mol. Biol. 338*, 77–91.

(23) Sklenár, V., Miyashiro, H., Zon, G., Miles, T., and Bax, A. (1986) Assignment of the ^{31}P and ^{1}H resonances in oligonucleotides by two-dimensional NMR spectroscopy. *FEBS Lett. 208*, 94–98.

(24) Goddard, T. D., and Kneller, D. G. (2008) *SPARKY 3*, University of California, San Francisco.

(25) Bax, A., Tjandra, N., and Zhengrong, W. (2001) Measurements of ^{1}H-^{31}P dipolar couplings in a DNA oligonucleotide by constant time NOESY difference spectroscopy. *J. Mol. Biol. 19*, 367–270.

(26) Case, D. A., Darden, T. A., Cheatham, T. E., III, Simmerling, C. L., Wang, J., Duke, R. E., Luo, R., Merz, K. M., Pearlman, D. A., Crowley, M., Walker, R. C., Zhang, W., Wang, B., Hayik, S., Roitberg, A., Seabra, G., Wong, K. F., Paesani, F., Wu, X., Brozell, S., Tsui, V., Gohlke, H., Yang, L., Tan, C., Mongan, J., Hornak, V., Cui, G., Beroza, P., Mathews, D. H., Schafmeister, C., Ross, W. S., and Kollman, P. A. (2006) *AMBER 9*, University of California, San Francisco.

(27) Summers, J. S., Roe, D., Boyle, P. D., Colvin, M., and Shaw, B. R. (1998) Structural Studies of a Borane-Modified Phosphate Diester Linkage: Ab Initio Calculations on the Dimethylboranophsphate Anion and the Single-Crystal X-ray Structure of Its Diisopropylammonium Salt. *Inorg. Chem. 37*, 4158–4159.

(28) Frisch, M. J., Trucks, G. W., Schlegel, H. B., Scuseria, G. E., Robb, M. A., Cheeseman, J. R., Montgomery, J. A., Jr., Vreven, T., Kudin, K. N., Burant, J. C., Millam, J. M., Iyengar, S. S., Tomasi, J., Barone, V., Mennucci, B., Cossi, M., Scalmani, G., Rega, N., Petersson, G. A., Nakatsuji, H., Hada, M., Ehara, M., Toyota, K., Fukuda, R., Hasegawa, J., Ishida, M., Nakajima, T., Honda, Y., Kitao, O., Nakai, H., Klene, M., Li, X., Knox, J. E., Hratchian, H. P., Cross, J. B., Bakken, V., Adamo, C., Jaramillo, J., Gomperts, R., Stratmann, R. E., Yazyev, O., Austin, A. J., Cammi, R., Pomelli, C., Ochterski, J. W., Ayala, P. Y., Morokuma, K., Voth, G. A., Salvador, P., Dannenberg, J. J., Zakrzewski, V. G., Dapprich, S., Daniels, A. D., Strain, M. C., Farkas, O., Malick, D. K., Rabuck, A. D., Raghavachari, K., Foresman, J. B., Ortiz, J. V., Cui, Q., Baboul, A. G., Clifford, S., Cioslowski, J., Stefanov, B. B., Liu, G., Liashenko, A., Piskorz, P., Komaromi, I., Martin, R. L., Fox, D. J., Keith, T., Al-Laham, M. A., Peng, C. Y., Nanayakkara, A., Challacombe, M., Gill, P. M. W., Johnson, B., Chen, W., Wong, M. W., Gonzalez, C., and Pople, J. A. (2004) *Gaussian 03*, revision C.02, Gaussian Inc., Wallingford, CT.

(29) Dupradeau, F.-Y., Pigache, A., Zaffran, T., Savineau, C., Lelong, R., Grivel, N., Lelong, D., Rosanski, W., and Cieplak, P. (2010) The R.E. D. tools: Advances in RESP and ESP charge derivation and force field library building. *Phys. Chem. Chem. Phys. 12*, 7821–7839.

(30) Pigache, A., Cieplak, P., and Dupradeau, F.-Y. (2004) Automatic and highly reproducible RESP and ESP charge derivation: Application to the development of programs RED and X RED. 227th ACS National Meeting, Anaheim, CA, March 28−April 1.

(31) (a) Keepers, J. W., and James, T. L. (1984) Two-dimensional nuclear Overhauser effect spectra. *J. Magn. Reson. 57*, 404–426. (b) Borgias, B. A., and James, T. L. (1988) COMATOSE, a method for constrained refinement of macro- molecular structure based on two-dimensional nuclear Overhauser effect spectra. *J. Magn. Reson. 79*, 493–512. (c) Thomas, P. D., Basus, V. J., and James, T. L. (1991) Protein solution structure determination using distances from two-dimensional nuclear Overhauser effect experiments: Effect of approximations on the accuracy of derived structures. *Proc. Natl. Acad. Sci. U.S. A. 88*, 1237–1241.

(32) (a) Borgias, B. A., and James, T. L. (1989) Two-dimensional nuclear Overhauser effect: Complete relaxation matrix analysis. *Methods Enzymol. 176*, 169–183. (b) Borgias, B. A., and James, T. L. (1990) MARDIGRAS: A procedure for matrix analysis of relaxation for discerning geometry of an aqueous structure. *J. Magn. Reson. 87*, 475–487.

(33) Rinkel, L. J., and Altona, C. (1987) Conformational analysis of the deoxyribofuranose ring in DNA by means of sums of proton-proton coupling constants: A graphical method. *J. Biomol. Struct. Dyn. 4*, 621–649.

(34) Mujeeb, A., Kerwin, S. M., and Kenyon, G. L. (1993) Solution Structure of a Conserved DNA Sequence from the HIV-1 Genome: Restrained Molecular Dynamics Simulation with Distance and Torsion Angle Restraints Derived from Two-Dimensional NMR Spectra. *Biochemistry 32*, 13419–13431.

(35) Blackburn, G. M., Gait, M. J., Loakes, D., and Williams, M. D. (2006) *Nucleic Acids in Chemistry and Biology*, 3rd ed., The Royal Society of Chemistry, Cambridge, U.K.

(36) Humphrey, W., Dalke, A., and Schulten, K. (1996) VMD: Visual Molecular Dynamics. *J. Mol. Graphics 14*, 33–38.

(37) Lavery, R., and Sklenar, H. (1996) *CURVES 5.1. Helical Analysis of Irregular Nucleic Acids*, Laboratoire de Biochimie Theorique CNRS, Paris.

(38) Wüthrich, K. (1986) *NMR of Proteins and Nuclic Acids*, Wiley-Interscience, New York.

(39) Gorenstein, D. G., Schroeder, S. A., Fu, J. M., Metz, J. T., Roongta, V., and Jones, C. R. (1998) Assignments of ^{31}P NMR Resonances in Oligodeoxyribonucleotides: Origin of Sequence-Specific Variations in the Deoxyribose Phosphate Backbone Conformation and the ^{31}P Chemical Shifts of Double-Helical Nucleic Acids. *Biochemistry 27*, 7223–7237.

(40) Li, P., Sergueeva, Z. A., Dobrikov, M., and Shaw, B. R. (2007) Nucleoside and Oligonucleoside Boranophosphates: Chemistry and Properties. *Chem. Rev. 107*, 4746–4796.

(41) Hantz, E., Larue, V., Ladam, P., Moyec, L. L., Gouyette, C., and Dinh, T. H. (2001) Solution conformation of an RNA−DNA hybrid duplex containing a pyrimidine RNA strand and a purine DNA strand. *Int. J. Biol. Macromol. 28*, 273–284.

(42) Gewirtz, A. M. (2000) Oligonucleotide Therapeutics: A Step Forward. *J. Clin. Oncol. 18*, 1809–1811.

(43) Coppelli, F. M., and Grandis, J. R. (2005) Oligonucleotides as anticancer agents: From the benchside to the clinic and beyond. *Curr. Pharm. Des. 11*, 2825–2840.

(44) Cerritelli, S. M., and Crouch, R. J. (2009) Ribonuclease H: The enzymes in eukaryotes. *FEBS J. 276*, 1495–1505.